

## A Unique Example of Structural and Magnetic Diversity in Four Interconvertible Copper(II)–Azide Complexes with the Same Schiff Base Ligand: A Monomer, a Dimer, a Chain, and a Layer

Subrata Naiya,<sup>†</sup> Chaitali Biswas,<sup>†,‡</sup> Michael G. B. Drew,<sup>§</sup> Carlos J. Gómez-García,<sup>\*,†,⊥</sup> Juan M. Clemente-Juan,<sup>⊥,||</sup> and Ashutosh Ghosh<sup>\*,†</sup>

<sup>†</sup>Department of Chemistry, University College of Science, University of Calcutta, 92, APC Road, Kolkata-700 009, India, <sup>‡</sup>Sarojini Naidu College for Women, 30 Jessore Road, Kolkata-700 028, India,

<sup>§</sup>School of Chemistry, The University of Reading, P.O. Box 224, Whiteknights, Reading RG 66AD, U.K.,

<sup>⊥</sup>Instituto de Ciencia Molecular (ICMol), Parque Científico, Universidad de Valencia, 46980 Paterna, Valencia, Spain, and <sup>||</sup>Fundación General de la Universidad de Valencia (FGUV), Valencia, Spain

Received March 23, 2010

Four new Cu(II)-azido complexes of formula [CuL(N<sub>3</sub>)] (**1**), [CuL(N<sub>3</sub>)<sub>2</sub>] (**2**), [Cu<sub>7</sub>L<sub>2</sub>(N<sub>3</sub>)<sub>12</sub>]<sub>n</sub> (**3**), and [Cu<sub>2</sub>L(dmen)(N<sub>3</sub>)<sub>3</sub>]<sub>n</sub> (**4**) (dmen = *N,N*-dimethylethylenediamine) have been synthesized using the same tridentate Schiff base ligand HL (2-[1-(2-dimethylaminoethylimino)ethyl]phenol, the condensation product of dmen and 2-hydroxyacetophenone). The four compounds have been characterized by X-ray structural analyses and variable-temperature magnetic susceptibility measurements. Complex **1** is mononuclear, whereas **2** is a single  $\mu$ -1,1 azido-bridged dinuclear compound. The polymeric compound **3** possesses a 2D structure in which the Cu(II) ions are linked by phenoxo oxygen atoms and two different azide bridges ( $\mu$ -1,1 and  $\mu$ -1,1,3). The structure of complex **4** is a double helix in which two  $\mu$ -1,3-azido-bridged alternating one-dimensional helical chains of CuL(N<sub>3</sub>) and Cu(dmen)(N<sub>3</sub>)<sub>2</sub> are joined together by weak  $\mu$ -1,1 azido bridges and H-bonds. The complexes interconvert in solution and can be obtained in pure form by carefully controlling the conditions. The magnetic properties of compounds **1** and **2** show the presence of very weak antiferromagnetic exchange interactions mediated by a ligand  $\pi$  overlap ( $J = -1.77$ ) and by an asymmetric 1,1-N<sub>3</sub> bridge ( $J = -1.97 \text{ cm}^{-1}$ ), respectively. Compound **3** presents, from the magnetic point of view, a decorated chain structure with both ferro- and antiferromagnetic interactions. Compound **4** is an alternating helicoidal chain with two weak antiferromagnetic exchange interactions ( $J = -1.35$  and  $-2.64 \text{ cm}^{-1}$ ).

### Introduction

The rational design and synthesis of polynuclear coordination complexes is an area of continuing interest in order to understand the structural and chemical factors that govern the exchange coupling between paramagnetic centers and to establish magnetostructural correlations in molecular systems with the aim of controlling and developing new functional molecular-based materials.<sup>1</sup> Although many different bridging groups and transition metal ions have been employed for

the construction of such species, the Cu(II)-azide system is one of the most popular among synthetic chemists. A variety of copper-azido complexes with discrete or one-, two-, and three-dimensional polymeric structures have been reported, in which the azido ligand exhibits diverse bridging modes ranging from  $\mu$ -1,1 (end-on, EO) and  $\mu$ -1,3 (end-to-end, EE) to  $\mu$ -1,1,1,  $\mu$ -1,1,3,  $\mu$ -1,1,1,1,  $\mu$ -1,1,3,3, and  $\mu$ -1,1,1,3,3,3, depending upon the steric and electronic demands of the co-ligands<sup>2–4</sup> (Scheme 1). This diversity in the structures of

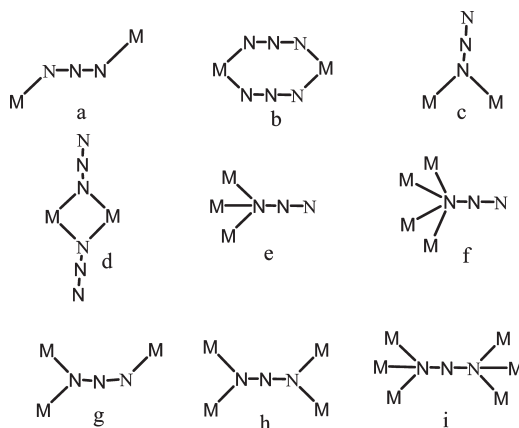
\*To whom correspondence should be addressed. E-mail: carlos.gomez@uv.es; ghosh\_59@yahoo.com.

(1) (a) Kostakis, G. E.; Powell, A. K. *Coord. Chem. Rev.* **2009**, *253*, 2686. (b) Ambrosi, G.; Formica, M.; Fusi, V.; Giorgi, L.; Micheloni, M. *Coord. Chem. Rev.* **2008**, *252*, 112. (c) Biswas, B.; Pieper, U.; Weyhermüller, T.; Chaudhuri, P. *Inorg. Chem.* **2009**, *48*, 6781. (d) Stamatatos, T. C.; Christou, G. *Inorg. Chem.* **2009**, *48*, 3308. (e) Baca, S. G.; Malaestean, I. L.; Keene, T. D.; Adams, H.; Ward, M. D.; Hauser, J.; Neels, A.; Decurtins, S. *Inorg. Chem.* **2008**, *47*, 11108. (f) Suárez-Varela, J.; Mota, A. J.; Aouryaghal, H.; Cano, J.; Rodríguez-Diéguez, A.; Luneau, D.; Colacio, E. *Inorg. Chem.* **2008**, *47*, 8143. (g) Biswas, C.; Mukherjee, P.; Drew, M. G. B.; Gómez-García, C. J.; Clemente-Juan, J. M.; Ghosh, A. *Inorg. Chem.* **2007**, *46*, 10771.

(2) (a) Stamatatos, T. C.; Papaefstathiou, G. S.; MacGillivray, L. R.; Escuer, A.; Vicente, R.; Ruiz, E.; Perlepes, S. P. *Inorg. Chem.* **2007**, *46*, 8843. (b) Gao, E.-Q.; Bai, S.-Q.; Wang, C.-F.; Yue, Y.-F.; Yan, C.-H. *Inorg. Chem.* **2003**, *42*, 8456. (c) Abu-Youssef, M. A. M.; Escuer, A.; Mautner, F. A.; Öhrström, L. *Dalton Trans.* **2008**, 3553.

(3) (a) You, Y. S.; Yoon, J. H.; Kimb, H. C.; Hong, C. S. *Chem. Commun.* **2005**, 4116. (b) Nanda, P. K.; Aromib, G.; Ray, D. *Chem. Commun.* **2006**, 3181. (c) Lazari, G.; Stamatatos, T. C.; Raptopoulou, C. P.; Psycharis, V.; Pissas, M.; Perlepes, S. P.; Boudalis, A. K. *Dalton Trans.* **2009**, 3215. (d) Lorosch, J.; Paulus, H.; Haase, W. *Inorg. Chim. Acta* **1985**, *106*, 101. (e) Boudalis, A. K.; Sanakis, Y.; Clemente-Juan, J. M.; Donnadieu, B.; Nastopoulos, V.; Mari, A.; Coppel, Y.; Tchuagues, J.-P.; Perlepes, S. P. *Chem.—Eur. J.* **2008**, *14*, 2514, and references therein.

Scheme 1. Various Azido Bridging Modes



the Cu(II) systems is a result of its flexibility in coordination numbers (ranging from 4 to 6) and geometry,<sup>2–4</sup> and taken together with its interesting magnetic properties, Cu(II) has therefore become the metal ion of choice for such studies. As a result of the extensive research of the last two decades, the superexchange mechanisms through various bridging modes of azide are now well established. For example, symmetric  $\mu$ -1,3 Cu(II) azide complexes are strongly antiferromagnetic, whereas Cu(II) complexes with double symmetric  $\mu$ -1,1 azide bridges are strongly ferromagnetic, provided that the Cu–N<sub>azide</sub>–Cu angle is less than 108°. Usually asymmetric  $\mu$ -1,3 azido bridges lead to weak antiferromagnetic coupling, whereas asymmetric  $\mu$ -1,1 azide bridges propagate weak to moderately strong ferro- or antiferromagnetic interactions.<sup>5c–e,i–k</sup> Since other structural parameters certainly affect magnetic exchange, a number of exceptions have been reported, and it has been pointed out that other structural parameters such as Cu–N bond lengths and the Cu(N)<sub>2</sub>Cu dihedral angles<sup>5</sup> need also to be considered.

On the contrary, the many possible bridging modes of azide and the flexible coordination number (and geometry) of Cu(II) make the synthesis of tailored compounds a real challenge for coordination chemists and crystal engineers. There are very few studies focusing on the variables that dictate the isolation of a particular polynuclear species. A common strategy for the synthesis of polynuclear complexes is to choose the blocking ligand in such a way that the copper

ion remains coordinately unsaturated and thus allows the azide to bridge the copper centers. Recently it has been shown that in neutral Cu-azido systems with chelating diamine ligands the dimensionalities of the polynuclear structures are determined by the relative molar quantities of copper and the diamine ligands.<sup>6</sup> The products, however, more often than not, are unexpected and result from uncontrolled self-assembly. In order to truly design the synthesis of a desired polynuclear material, one should have a clear knowledge regarding the synthetic conditions that lead to the formation of a particular product and/or the interconversion between the products. To the best of our knowledge, in the Cu-azide system, apart from attempts of changing the molar proportions,<sup>6</sup> the effects of other factors (e.g., temperature, template effect of the counteranions, solvents, etc.) that are well known to modulate the structure of compounds in several other systems<sup>7</sup> have not been studied systematically until the present work. Herein, we report the synthesis, structural characterization, and variable-temperature magnetic behavior of four new compounds: a mononuclear [CuL(N<sub>3</sub>)] (**1**), a single  $\mu$ -1,1-azido-bridged dinuclear [CuL(N<sub>3</sub>)<sub>2</sub>] (**2**), a 2D coordination polymer with  $\mu$ -1,1 and  $\mu$ -1,1,3 azide bridges [Cu<sub>7</sub>L<sub>2</sub>(N<sub>3</sub>)<sub>12</sub>] (**3**), and a  $\mu$ -1,3- and  $\mu$ -1,1-azido-bridged double-stranded helix, [Cu<sub>2</sub>L(dmen)(N<sub>3</sub>)<sub>3</sub>] (**4**). All four complexes have been prepared using the same N,N,O donor Schiff base ligand (2-[1-(2-dimethylaminoethylimino)ethyl]phenol) (HL), the condensation product of *N,N*-dimethyl-1,2-diaminoethane (dmen) and 2-hydroxyacetophenone (Scheme 1) by varying the reaction conditions. The factors that allow the conversion of one compound into another have also been explored in detail. During the course of this work, the crystal structure and magnetic properties of compound **4** have been reported by others.<sup>8</sup> However, the previous authors reported just one compound formed with this ligand and as a result did not study any possible interconversion to related compounds. Therefore, we retain mention of this compound in our paper, as it is an integral part of the interconversion of the compounds, but do not describe the structure in detail. Moreover, we fit the magnetic data of this compound with a different model and obtain a better fit, which is also reported here.

## Experimental Section

**Materials.** The reagents and solvents used were of commercially available reagent quality.

**Synthesis of the Schiff Base Ligand HL** [(2-[1-(2-dimethylaminoethylimino)ethyl]phenol)]. The monocondensed Schiff base ligand HL (Scheme 2) has been synthesized as reported before.<sup>8–10</sup> A

(4) (a) Goher, M. A. S.; Mautner, F. A. *Polyhedron* **1995**, *14*, 1439. (b) Gu, Z.-G.; Xu, Y.-F.; Yin, X.-J.; Zhou, X.-H.; Zuo, J.-L.; You, X.-Z. *Dalton Trans.* **2008**, 5593. (c) Zhang, X.-M.; Zhao, Y.-F.; Wu, H.-S.; Battenb, S. R.; Ng, S. W. *Dalton Trans.* **2006**, 3170. (d) Guo, G. C.; Mak, T. C. W. *Angew. Chem., Int. Ed.* **1998**, *37*, 3268.

(5) (a) Tandon, S. S.; Thompson, L. K.; Manuel, M. E.; Bridson, J. N. *Inorg. Chem.* **1994**, *33*, 5555. (b) Ribas, J.; Escuer, A.; Monfort, M.; Vicente, R.; Cortes, R.; Lezama, L.; Rojo, T. *Coord. Chem. Rev.* **1999**, *193–195*, 1027. (c) Koner, S.; Saha, S.; Mallah, T.; Okamoto, K.-I. *Inorg. Chem.* **2004**, *43*, 840. (d) Zbiri, M.; Saha, S.; Adhikary, C.; Chaudhuri, S.; Daul, C.; Koner, S. *Inorg. Chim. Acta* **2006**, *359*, 1193. (e) Mukherjee, P. S.; Dalai, S.; Mostafa, G.; Lu, T.-H.; Rentschler, E.; Chaudhuri, N. R. *New J. Chem.* **2001**, *25*, 1203. (f) Manikandan, P.; Muthukumar, R.; Justin Thomas, K. R.; Varghese, B.; Chandramouli, G. V. R.; Manoharan, P. T. *Inorg. Chem.* **2001**, *40*, 2378. (g) Dey, S. K.; Mondal, N.; Fallah, M. S. E.; Vicente, R.; Escuer, A.; Solans, X. Font-Bardia, M.; Matsushita, T.; Gramlich, V.; Mitra, S. *Inorg. Chem.* **2004**, *43*, 2427. (h) Mukherjee, P. S.; Maji, T. K.; Mostafa, G.; Mallah, T.; Chaudhuri, N. R. *Inorg. Chem.* **2000**, *39*, 5147. (i) Comarmond, P.; Plumere, P.; Lehn, J. M.; Augus, Y.; Louis, R.; Weiss, R.; Kahn, O.; Morgenstern-Badarau, I. *J. Am. Chem. Soc.* **1982**, *104*, 6330. (j) Ray, M. S.; Ghosh, A.; Bhattacharya, R.; Mukhopadhyay, G.; Drew, M. G. B.; Ribas, J. *Dalton Trans.* **2004**, 252. (k) Ray, M. S.; Ghosh, A.; Chaudhuri, S.; Drew, M. G. B.; Ribas, J. *Eur. J. Inorg. Chem.* **2004**, 3110.

(6) (a) Mondal, K. C.; Mukherjee, P. S. *Inorg. Chem.* **2008**, *47*, 4215. (b) Mukherjee, S.; Gole, B.; Chakrabarty, R.; Mukherjee, P. S. *Inorg. Chem.* **2009**, *48*, 11325.

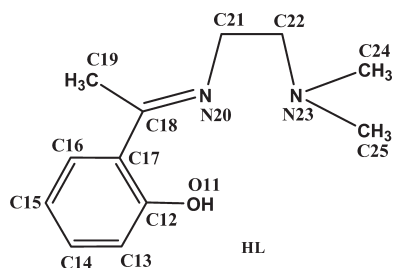
(7) (a) Hu, X.-X.; Xu, J.-Q.; Cheng, P.; Chen, X.-Y.; Cui, X.-B.; Song, J.-F.; Yang, G.-D.; Wang, T.-G. *Inorg. Chem.* **2004**, *43*, 2261. (b) Withersby, M. A.; Blake, A. J.; Champness, N. R.; Cooke, P. A.; Hubbert, P.; Li, W.-S.; Schröder, M. *Inorg. Chem.* **1999**, *38*, 2259. (c) Forster, P. M.; Burbank, A. R.; Livage, C.; Férey, G.; Cheetham, A. K. *Chem. Commun.* **2004**, 368. (d) Tong, M.-L.; Kitagawa, S.; Changa, H.-C.; Ohba, M. *Chem. Commun.* **2004**, 418. (e) Mukherjee, P.; Drew, M. G. B.; Gómez-García, C. J.; Ghosh, A. *Inorg. Chem.* **2009**, *48*, 5848.

(8) Adhikary, C.; Sen, R.; Tuchagues, J.-P.; Chaudhuri, S.; Ianelli, S.; Solzi, M.; Koner, S. *Inorg. Chim. Acta* **2009**, *362*, 5211.

(9) Biswas, C.; Drew, M. G. B.; Asthana, S.; Desplanches, C.; Ghosh, A. *J. Mol. Struct.* **2010**, *965*, 39.

(10) Talukder, P.; Sen, S.; Mitra, S.; Dahlenberg, L.; Desplanches, C.; Sutter, J.-P. *Eur. J. Inorg. Chem.* **2006**, 329.

Scheme 2. Schiff Base Ligand



solution of 2-hydroxyacetophenone (20 mmol, 2.41 mL) and *N,N*-dimethyl-1,2-diaminoethane (20 mmol, 2.20 mL) in methanol (50 mL) was refluxed for one hour. The resulting dark yellow solution was then used directly for complex formation. The ligand was isolated as a yellow solid by removing methanol completely from the resultant solution under vacuum to result in a viscous liquid, followed by addition of a mixture of petroleum ether and chloroform. The ligand was characterized by elemental analyses and  $^1\text{H}$  NMR study.

Ligand (HL). Anal. Calcd for  $\text{C}_{12}\text{H}_{18}\text{N}_2\text{O}$ : C, 69.87; H, 8.80; N, 13.58. Found: C, 69.81; H, 8.89; N, 13.45.  $^1\text{H}$  NMR ( $\text{CDCl}_3$ , 300 MHz) (Figure S1): 2.11 (s, 3H,  $\text{CH}_3$ ); 2.28 (s, 6H,  $2 \times \text{N-CH}_3$ ); 2.65 (t,  $J = 6.9$  Hz, 2H,  $\text{CH}_2$ ); 3.61 (t,  $J = 6.9$  Hz, 2H,  $\text{CH}_2$ ); 6.87 (dd,  $^3J = 8.4$  Hz and  $^4J = 0.9$  Hz, 1H,  $\text{C13-H}$ ); 7.22 (dt,  $^3J = 8.7$  Hz and  $^4J = 1.5$  Hz,  $\text{C14-H}$ ); 6.70 (dt,  $^3J = 8.1$  and  $^4J = 1.2$  Hz, 1H,  $\text{C15-H}$ ); 7.44 (dd,  $^3J = 8.1$  Hz and  $^4J = 1.5$  Hz, 1H,  $\text{C16-H}$ ); 16.38 (s, 1H, OH).

**Synthesis of the Complexes  $[\text{CuL}(\text{N}_3)]$  (1) and  $[\text{CuL}(\text{N}_3)]_2$  (2).** To a 30 mL methanolic solution of  $\text{Cu}(\text{ClO}_4)_2 \cdot 6\text{H}_2\text{O}$  (5.00 mmol, 1.828 g) and the HL (5.00 mmol) was added an aqueous solution (1 mL) of  $\text{NaN}_3$  (5.00 mmol; 0.325 g). The mixture was stirred for 2 h and filtered. The filtrate was then divided into two equal parts; one of the parts was kept at room temperature and the other was kept in a refrigerator ( $-10^\circ\text{C}$ ). Thin, deep-blue-colored, block-shaped single crystals of **1** were obtained after 2 days from the filtrate which was kept at room temperature, whereas dark blue, needle-shaped, single crystals of **2** were obtained after one week from the other part of the filtrate which was kept in the refrigerator. Crystals of **1** and **2** were suitable for X-ray analysis.

Compound **1**. Yield: 0.56 g, 72%. Anal. Calcd for  $\text{C}_{12}\text{H}_{17}\text{CuN}_5\text{O}$ : C, 46.37; H, 5.51; N, 22.53. Found: C, 46.21; H, 5.66; N, 22.42. IR (KBr,  $\text{cm}^{-1}$ ): 3363  $\nu(\text{N-H})$ , 1594  $\nu(\text{C=N})$ , 2044  $\nu(\text{N-N})$ ,  $\lambda_{\text{max}}$  (nm) [ $\epsilon_{\text{max}}$  ( $\text{dm}^3 \text{mol}^{-1} \text{cm}^{-1}$ )] (methanol), 603 nm (66).

Compound **2**. Yield: 0.52 g, 67%. Anal. Calcd for  $\text{C}_{24}\text{H}_{34}\text{Cu}_2\text{N}_{10}\text{O}_2$ : C, 46.37; H, 5.51; N, 22.53. Found: C, 46.31; H, 5.46; N, 22.68. IR (KBr,  $\text{cm}^{-1}$ ): 3364  $\nu(\text{N-H})$ , 1594  $\nu(\text{C=N})$ , 2046  $\nu(\text{N-N})$ ,  $\lambda_{\text{max}}$  (nm) [ $\epsilon_{\text{max}}$  ( $\text{dm}^3 \text{mol}^{-1} \text{cm}^{-1}$ )] (methanol), 594 nm (114).

**Synthesis of the Complex  $[\text{Cu}_2\text{L}_2(\text{N}_3)_{12}]_n$  (3).** To a 30 mL methanolic solution of  $[\text{Cu}_2(\text{OAc})_4 \cdot (\text{H}_2\text{O})_2]$  (7.00 mmol, 1.397 g) and HL (2.00 mmol) was added an aqueous solution (1 mL) of excess  $\text{NaN}_3$  (12.00 mmol, 0.780 g) with constant stirring. During stirring, a dark-blue-colored, fine crystalline precipitate of **3** was separated. The mixture was then filtered. Blue-colored, plate-shaped, diffraction quality single crystals of **3** were obtained after a few days on slow evaporation of the filtrate. The IR spectra of the fine crystalline precipitate and that of single crystals were identical.

Yield: 1.02 g, 75%. Anal. Calcd for  $\text{C}_{24}\text{H}_{34}\text{Cu}_2\text{N}_{40}\text{O}_2$ : C, 21.20; H, 2.52; N, 41.21. Found: C, 21.33; H, 2.42; N, 41.11. IR (KBr,  $\text{cm}^{-1}$ ): 3361  $\nu(\text{N-H})$ , 1587  $\nu(\text{C=N})$ , 2062–2085  $\nu(\text{N-N})$ ,  $\lambda_{\text{max}}$  (nm) [ $\epsilon_{\text{max}}$  ( $\text{dm}^3 \text{mol}^{-1} \text{cm}^{-1}$ )] (methanol), 599 (189).

**Synthesis of the Complex  $[\text{Cu}_2\text{L}(\text{dmen})(\text{N}_3)_3]_n$  (4).** The procedure was similar to that for complex **3**. An aqueous solution of excess  $\text{NaN}_3$  (15 mmol, 0.780 g) was added, with constant stirring, to a methanolic solution of  $\text{Cu}(\text{ClO}_4)_2 \cdot 6\text{H}_2\text{O}$  (7.00 mmol, 2.559 g) (instead of  $[\text{Cu}_2(\text{OAc})_4 \cdot (\text{H}_2\text{O})_2]$  for **3**) and HL (2 mmol). The mixture was then refluxed for one hour. The resulting solution was left to stand overnight in air, when plate-

shaped, blue-colored, X-ray quality single crystals of complex **4** appeared at the bottom of the vessel.

Yield: 0.10 g, 19%. Anal. Calcd for  $\text{C}_{16}\text{H}_{29}\text{Cu}_2\text{N}_{13}\text{O}$ : C, 35.16; H, 5.35; N, 33.31. Found: C, 35.09; H, 5.45; N, 33.23. IR (KBr,  $\text{cm}^{-1}$ ): 3126, 3217, and 348  $\nu(\text{N-H})$ , 1598  $\nu(\text{C=N})$ , 2036  $\nu(\text{N-N})$ ,  $\lambda_{\text{max}}$  (nm) [ $\epsilon_{\text{max}}$  ( $\text{dm}^3 \text{mol}^{-1} \text{cm}^{-1}$ )] (methanol), 612 (203).

The complex was also prepared in much higher yield (0.43 g, 78%) by adding a methanol solution (20 mL) of HL and dmen (2 mmol each) to a methanol solution (10 mL) of  $\text{Cu}(\text{ClO}_4)_2 \cdot 6\text{H}_2\text{O}$  (1.462 g, 4 mmol) followed by an aqueous solution (1 mL) of  $\text{NaN}_3$  (0.520 g, 8 mmol). The crystalline compound **4** started to separate within half an hour on keeping the mixture at room temperature. The product was collected after about 24 h.

**Physical Measurements.** Elemental analyses (C, H, and N) were performed using a Perkin-Elmer 240C elemental analyzer. IR spectra in KBr pellets ( $4500\text{--}500 \text{ cm}^{-1}$ ) were recorded using a Perkin-Elmer RXI FT-IR spectrophotometer. The  $^1\text{H}$  NMR spectra at 300 MHz were recorded in  $\text{CDCl}_3$  on a Bruker DRX 300 spectrometer. The numbers in parentheses after the H atoms in the NMR spectral data are the numbers of carbon atoms to which the hydrogen atoms are attached, as in Scheme 2. Electronic spectra in methanol (1000–200 nm) were recorded in a Hitachi U-3501 spectrophotometer. High-resolution mass spectra (HRMS) electrospray ionization (ESI) was recorded on a Qtof Micro YA263 high-resolution mass spectrometer. For HRMS (ESI), the sample was taken in  $\text{CH}_3\text{OH}$ . Thermal analyses (TG-DTA) were carried out on a Mettler Toledo TGA/SDTA 851 thermal analyzer in a dynamic atmosphere of dinitrogen (flow rate  $30 \text{ cm}^3 \text{min}^{-1}$ ). The samples were heated in an alumina crucible at a rate of  $10^\circ\text{C min}^{-1}$ . Variable-temperature magnetic susceptibility measurements were carried out in the temperature range 2–300 K with an applied magnetic field of 0.1 T on polycrystalline samples of compounds **1–4** (with masses of 51.70, 25.77, 39.14, and 41.39 mg, respectively) with a Quantum Design MPMS-XL-5 SQUID susceptometer. Isothermal magnetization measurements were performed on the same samples at 2 K with magnetic fields up to 5 T. The susceptibility data were corrected for the sample holders previously measured using the same conditions and for the diamagnetic contributions of the salt as deduced by using Pascal's constant tables ( $\chi_{\text{dia}} = -239.3 \times 10^{-6}$ ,  $-184.1 \times 10^{-6}$ ,  $-803.6 \times 10^{-6}$ , and  $-394.3 \times 10^{-6} \text{ emu} \cdot \text{mol}^{-1}$  for **1–4**, respectively).

**Crystallographic Studies.** Intensity data for the four compounds were collected with Mo K $\alpha$  radiation at 150 K using an Oxford Diffraction X-Calibur CCD system. The crystals were positioned at 50 mm from the CCD; 321 frames were measured with a counting time of 10 s. Data analyses were carried out with the CrysAlis program.<sup>11</sup> The structures were solved using direct methods with the Shelxs97 program.<sup>12</sup> The non-hydrogen atoms were refined with anisotropic thermal parameters. The hydrogen atoms bonded to carbon were included in geometric positions and given thermal parameters equivalent to 1.2 times (or 1.5 times for methyl hydrogen atoms) those of the atom to which they were attached. Absorption corrections were carried out using the ABSPACK program.<sup>13</sup> The structures were refined on  $F^2$  using Shelxl97.<sup>12</sup> Selected dimensions in the four complexes are given in Table 1.

## Results and Discussion

**Synthesis of the Complexes and Their Interconversion.** The monocondensed tridentate Schiff base ligand HL (2-[1-(2-dimethylaminoethylimino)ethyl]phenol) and its Cu(II) complexes with  $\text{ClO}_4^-$  and  $\text{BF}_4^-$  anions are

(11) CrysAlis; Oxford Diffraction Ltd.: Abingdon, U.K., 2006.

(12) Sheldrick, G. M. Shelxs97 and Shelxl97, Programs for Crystallographic Solution and Refinement. *Acta Crystallogr.* **2008**, *A64*, 112.

(13) ABSPACK; Oxford Diffraction Ltd: Oxford, U.K., 2005.



Table 1. Crystal Data and Structure Refinement of Complexes 1–4

	1	2	3	4
formula	C <sub>12</sub> H <sub>17</sub> CuN <sub>5</sub> O	C <sub>24</sub> H <sub>34</sub> Cu <sub>2</sub> N <sub>10</sub> O <sub>2</sub>	C <sub>24</sub> H <sub>34</sub> Cu <sub>7</sub> N <sub>40</sub> O <sub>2</sub>	C <sub>16</sub> H <sub>29</sub> Cu <sub>2</sub> N <sub>13</sub> O
fw	310.85	621.70	1359.69	546.62
space group	<i>Cc</i>	<i>P2<sub>1</sub>/n</i>	<i>P</i> $\bar{1}$	<i>C2/c</i>
cryst syst	monoclinic	monoclinic	triclinic	monoclinic
<i>a</i> /Å	19.635(3)	11.783(4)	10.3496(11)	24.928(5)
<i>b</i> /Å	12.194 (2)	19.194(5)	11.3763(10)	9.054(2)
<i>c</i> /Å	12.111(2)	12.154(3)	11.7155(10)	22.412(2)
$\alpha$ /deg	(90)	(90)	98.344(8)	(90)
$\beta$ /deg	107.06(2)	94.96(2)	115.39 (1)	119.75(1)
$\gamma$ /deg	(90)	(90)	98.852(8)	(90)
<i>V</i> /Å <sup>3</sup>	2772.2(7)	2738.4(13)	1196.4(2)	4391.7(14)
<i>Z</i>	8	4	1	8
calcd density (g·cm <sup>−3</sup> )	1.490	1.508	1.887	1.653
absorp coeff ( $\mu$ , mm <sup>−1</sup> )	1.575	1.595	3.127	1.976
<i>F</i> (000)	1288	1288	677	2256
cryst size (mm)	0.12 × 0.14 × 0.17	0.03 × 0.03 × 0.22	0.02 × 0.19 × 0.19	0.05 × 0.17 × 0.17
$\theta$ range (deg)	2.4, 30.0	2.5, 30.0	2.2, 30.0	2.44, 30.0
<i>R</i> (int)	0.052	0.326	0.080	0.062
total reflns	7860	18 932	8037	14 808
no. of unique data	5116	7928	6384	6365
data with <i>I</i> > 2 $\sigma$ ( <i>I</i> )	2462	2048	1907	4019
<i>R</i> <sub>1</sub> on <i>I</i> > 2 $\sigma$ ( <i>I</i> )	0.0848	0.1043	0.0839	0.0660
<i>wR</i> <sub>2</sub> on <i>I</i> > 2 $\sigma$ ( <i>I</i> )	0.2386	0.2023	0.1151	0.1622
GOF on <i>F</i> <sup>2</sup>	0.90	0.81	0.82	0.99

known,<sup>9,10</sup> both of which are aqua-bridged dinuclear compounds. In the present investigation, we have used this ligand for the synthesis of complexes with Cu(II)-azide. This group of mononegative N,N,O donor ligands is well known to produce mononuclear or dinuclear double asymmetric EO azide-bridged complexes.<sup>5c–e,7e,14–16</sup> Therefore, it is not surprising that the mononuclear compound **1** could be isolated as deep-blue-colored, block-shaped crystals by reacting a methanolic solution of Cu(ClO<sub>4</sub>)<sub>2</sub>·6H<sub>2</sub>O with a methanolic solution of HL in 1:1 molar ratio followed by the addition of aqueous solutions of NaN<sub>3</sub> at room temperature (25–35 °C) (Scheme 3). To study if temperature has any effect on the molecular structure, the same reaction mixture was kept in a refrigerator (ca. −10 °C) when dark-blue-colored, needle-shaped crystals of **2** appeared, having distinctly different morphology from that of **1**. Interestingly, compounds **1** and **2** are easily interconvertible: a methanolic solution of **1** or **2** after slow evaporation at room temperature yields compound **1**, but the same solution at low temperature (−10 °C) produces compound **2** (Scheme 3). The results clearly indicate that the crystallization temperature plays a crucial role in the final structure obtained. The HRMS-ESI of **1** and **2** recorded in methanolic solutions are identical (Figure S2, Supporting Information). The spectra show a less intense (42%) peak at ca. *m/z* 268, corresponding to the azide-free cationic species of the mononuclear complex [Cu(L)]<sup>+</sup>. The most intense (100%) peak observed, at ca. *m/z* 578, can be assigned to the association of two mononuclear species by a single azide ion, [Cu<sub>2</sub>L<sub>2</sub>(N<sub>3</sub>)]<sup>+</sup>.

On the other hand, when HL is allowed to react with excess [Cu<sub>2</sub>(OAc)<sub>4</sub>·(H<sub>2</sub>O)<sub>2</sub>] and azide ions (3:7) at room temperature, the 2D polymer [Cu<sub>7</sub>L<sub>2</sub>(N<sub>3</sub>)<sub>12</sub>] (**3**), which is

held together by azide bridges ( $\mu$ -1,1  $\mu$ -1,1,3), is obtained. Compound **3** is sparingly soluble in methanol at room temperature. In boiling methanol its solubility increases, and interestingly, this solution (obtained after separation of undissolved solid by filtration) yielded compound **1** on evaporation at room temperature, indicating that compound **3** converts in solution to compound **1** (as is evident from the mass spectra of the solution, identical to that of **1**). Even more surprising is the fact that compound **1** also converts into **3** in a rather easy way; when a methanolic solution of an excess of copper acetate and sodium azide is added to a methanolic solution of **1**, compound **3** starts to crystallize within an hour. The lower solubility of **3** seems to be the driving force in the equilibrium toward its formation. By contrast, when an excess of copper(II) salts other than copper acetate (perchlorate, nitrate, or chloride) and azide are allowed to react with HL at room temperature, compound **4** is formed along with **1**. However if the reaction mixture is refluxed and then allowed to stand at room temperature, compound **4** is the only product that crystallizes. The structure of compound **4** shows that it is an azide-bridged chain containing alternate Cu(L)(N<sub>3</sub>) and Cu(dmen)(N<sub>3</sub>)<sub>2</sub> moieties. The dmen ligand might come from the hydrolysis of the Schiff base ligand or from a small portion of unreacted dmen in the solution of HL used for complex formation. However, it is found that compound **1** can be converted into compound **4**, when a methanolic solution of **1** is reacted with excess copper perchlorate and azide. Therefore, hydrolysis of the Schiff base certainly takes place, but this is not very surprising, as metal ion catalyzed hydrolysis of Schiff bases is well documented in the literature.<sup>14,17,18</sup> Compound **4** transforms completely into **1** when 2-hydroxyacetophenone is added to a methanol solution of **4** (3:2 molar ratio) and the solution is refluxed for 1 h (Scheme 3).

(14) Mukherjee, P.; Drew, M. G. B.; Ghosh, A. *Eur. J. Inorg. Chem.* **2008**, 3372.

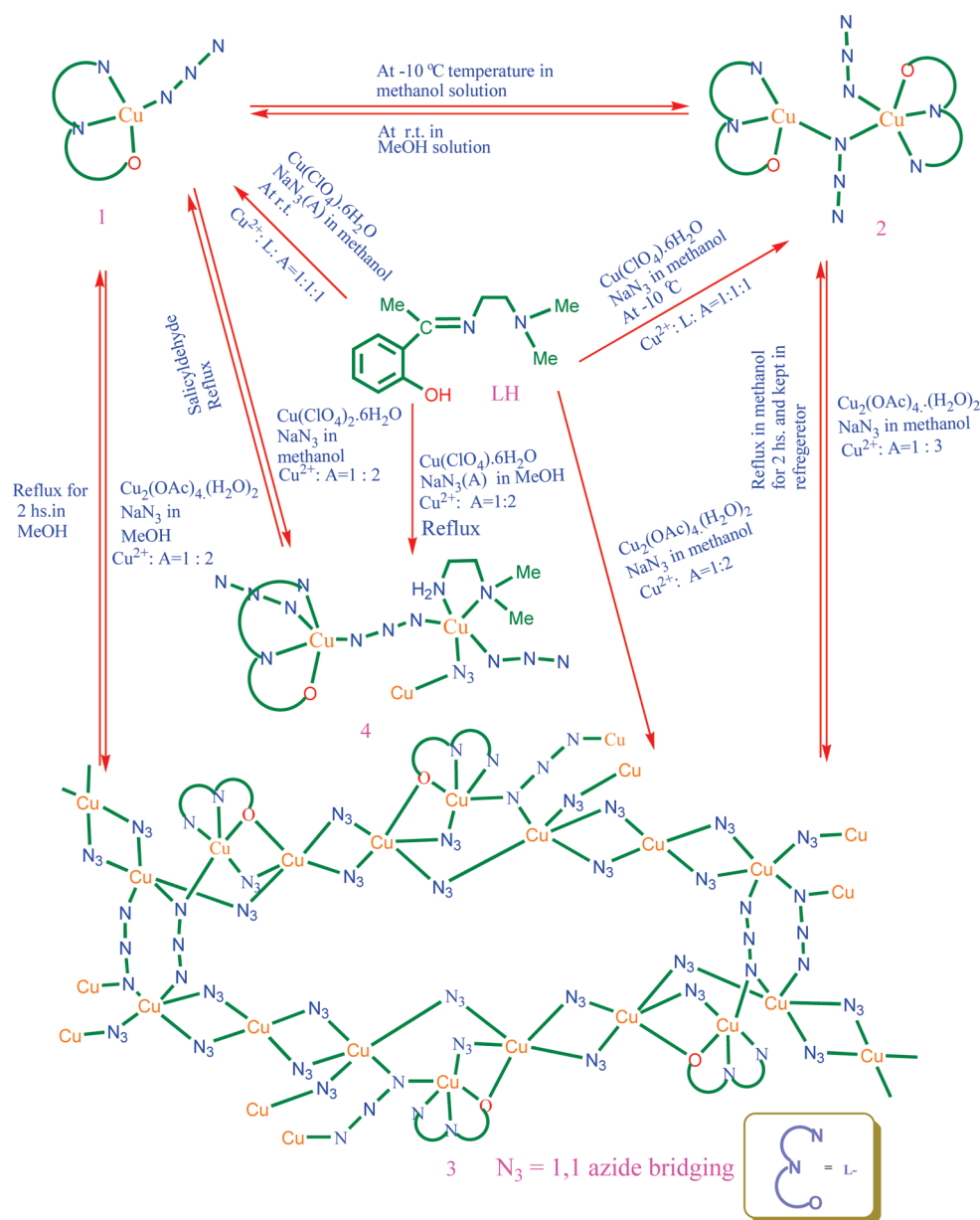
(15) (a) Jiang, Y.-B.; Kou, H.-Z.; Wang, R.-J.; Cui, A.-L. *Eur. J. Inorg. Chem.* **2004**, 4608. (b) You, Z.-L.; Jiao, Q.-Z.; Niu, S.-Y.; Chi, J.-Y. *Z. Anorg. Allg. Chem.* **2006**, 632, 2481.

(16) Talukder, P.; Datta, A.; Mitra, S.; Rosair, G.; Fallah, M. S. E.; Ribas, J. *Dalton Trans.* **2004**, 4161.

(17) Mandal, D.; Bertolasi, V.; Ribas-Ariño, J.; Aromí, G.; Ray, D. *Inorg. Chem.* **2008**, 47, 3465.

(18) Sarkar, B.; Ray, M. S.; Drew, M. G. B.; Figuerola, A.; Diaz, C.; Ghosh, A. *Polyhedron* **2006**, 25, 3084.

Scheme 3



The isolation of **3** in the presence of copper acetate but not of the other salts indicates that acetate ion definitely has an important role in its formation. One possibility is that the acetate ion helps to hold two Cu(II) ions together via a copper acetate dimer, thus facilitating the formation of the azido-bridged polynuclear structure **3** via a templating effect.

**IR and UV–Vis Spectra of Complexes.** Spectroscopic data and their assignments are given in the Experimental Section. The IR spectra of the complexes are similar and show strong sharp peaks for  $\nu(\text{C}=\text{N})$  at 1594, 1594, 1587, and 1598  $\text{cm}^{-1}$  for complexes **1–4** respectively, confirming the presence of the Schiff base. Two sharp peaks at 3217 and 3126  $\text{cm}^{-1}$  for complex **4** are attributed to the presence of a free amine group, which is produced by the hydrolysis of the Schiff base ligand, consistent with the single-crystal X-ray structure. The peaks at 2044 and 2046  $\text{cm}^{-1}$  in the IR spectra of **1** and **2**, respectively, appear to be due to the stretching of the terminal or  $\mu$ -1,1

azide bridge, while two overlapping but distinct peaks at 2062 to 2085  $\text{cm}^{-1}$  for complex **3** corroborate the presence of two types of azido bridging ( $\mu$ -1,1, and  $\mu$ -1,1,3) in the complex. Complex **4** shows a broad and single peak at 2036  $\text{cm}^{-1}$ . The electronic spectra in methanolic solution of the four complexes display a single absorption band at 603, 594, 599, and 612 nm for complexes **1–4**, respectively. These spectra are typical of a square-based environment for Cu(II).

**Structure of  $[\text{Cu}(\text{L})(\text{N}_3)]$  (**1**).** In **1**, there are two discrete molecules of  $[\text{Cu}(\text{L})(\text{N}_3)]$ , called **A** and **B** in the asymmetric unit, which have equivalent structures. The structure of **1A** is shown in Figure 1 together with the numbering scheme in the metal coordination sphere. Bond distances and bond angles are given in Table 2. Both molecules, **1A** and **1B**, contain a Cu(II) atom in a four-coordinate square-planar geometry bonded to the three donor atoms O11, N20, and N23 of the tridentate ligand **L** together with an azide nitrogen N1 with bond distances of 1.834(8),

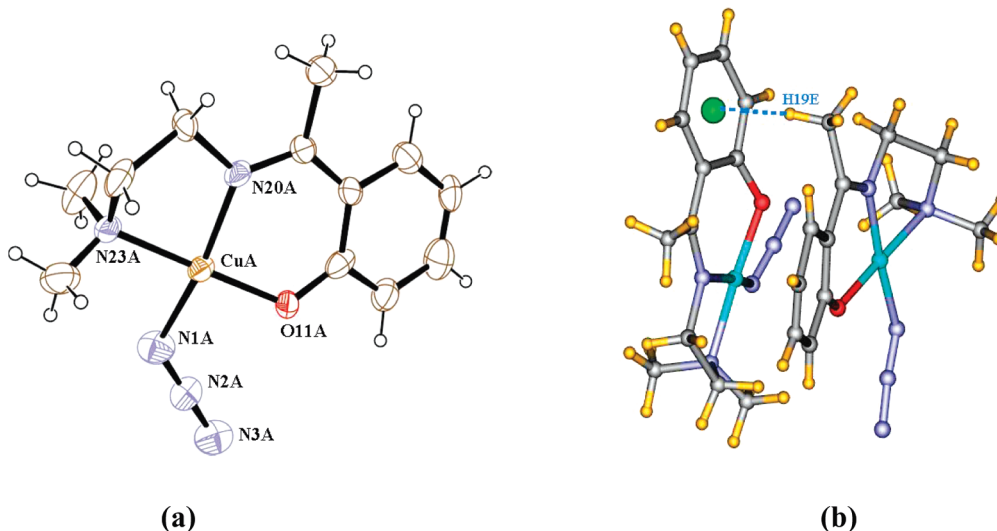


**Figure 1.** Structure of complex **1**. (a) Structure of **1A** with ellipsoids drawn at 30% probability. The structure of **1B** is equivalent. (b) Dimeric structure formed by a C–H/ $\pi$  interaction between molecules **1A** and **1B**.

**Table 2.** Selected Bond Lengths (Å) and Bond Angles (deg) for Complexes **1** and **2**

bond	<b>1A</b>	<b>1B</b>	<b>2A</b>	<b>2B</b>
Cu1–N1	1.932(14)	1.937(14)	1.946(8)	1.957(8)
Cu1–O11	1.834(8)	1.903(9)	1.917(6)	1.923(7)
Cu1–N20	1.976(9)	1.993(12)	1.918(8)	1.919(8)
Cu1–N23	1.981(11)	2.007(9)	2.064(8)	2.063(9)
O11–Cu1–N20	93.4(4)	91.0(5)	91.0(3)	92.6(3)
O11–Cu1–N23	175.0(4)	177.0(5)	163.5(3)	166.9(3)
N20–Cu1–N23	84.4(4)	87.5(5)	84.8(3)	85.1(3)
O11–Cu1–N1	92.9(5)	91.1(5)	93.1(3)	91.2(3)
N20–Cu1–N1	168.8(5)	176.0(6)	175.6(3)	169.9(3)
N23–Cu1–N1	89.9(5)	90.2(5)	90.9(3)	93.3(3)

1.976(9), 1.981(11), 1.932(14) Å and 1.903(9), 1.993(12), 2.007(9), 1.937(14) Å for **1A** and **1B**, respectively. In both molecules there are no significant interactions in axial positions, the closest contact being 3.28(1) Å for CuB to O11A (0.5+*x*, 0.5+*y*, 1+*z*). Deviations of donor atoms O11, N20, N23, and N1 from their mean plane are –0.116, 0.119, –0.119, and 0.116 Å, respectively, for **1A**, showing a tetrahedral distortion, whereas the four donor atoms are nearly coplanar in **1B**, with an rms deviation of 0.006 Å. The central Cu(II) atom deviates slightly from the basal plane by 0.044(6) Å in **1A** and 0.051(6) Å in **1B**. The tetrahedral distortion is apparent in **1A** since one pair of mutually trans donor atoms clearly lie below the plane while the other pair is above the plane with the metal ion nearly in the mean plane. The dihedral angles between the two planes (N1–Cu–O11 and N20–Cu–N23) are 10.58° for **1A** and 4.23° for **1B**. Each monomer, **1A** and **1B**, is stacked by a weak C–H/ $\pi$  interaction (Figure 1b). The C–H/ $\pi$  distance from C19–H19E of the methyl group of **1B** to the centroid of the phenyl ring (CG) of **1A** at symmetry operation 0.5+*x*, 0.5+*y*, 1+*z* is 2.91 Å with  $\gamma = 17.11^\circ$ .

**Structure of [Cu<sub>2</sub>L<sub>2</sub>(N<sub>3</sub>)<sub>2</sub>] (**2**).** The structure of **2**, Cu<sub>2</sub>L<sub>2</sub>(N<sub>3</sub>)<sub>2</sub>, also contains two copper atoms in the asymmetric unit (Figure 2a). Again the basal plane in both cases (**2A** and **2B**) consists of the three donor atoms O11, N20, and N23 of the Schiff base ligand together with an azide nitrogen atom, N1, at 1.917(6), 1.918(8), 2.064(8), 1.946(8) Å and 1.923(7), 1.919(8), 2.063(9), 1.957(8) Å from the Cu(II) atom in molecules **2A** and **2B**, respec-

tively. Bond distances and bond angles in the coordination spheres are given in Table 2. However in this case CuA has a weak axial interaction with atom N1B from an azide at 2.529(8) Å, thus forming a square-pyramidal coordination. The angles subtended by N1B with N1A, O11A, N20A, and N23A at the metal are 93.4(3)°, 94.5(3)°, 87.9(3)°, and 101.2(3)°, respectively, confirming that it is in an axial position. CuB shows no such axial interaction. Indeed the CuB–N1A distance is 3.585(11) Å and CuB is tetracoordinated with a square-planar environment. Deviations of donor atoms O11, N20, N23, and N1 from the mean plane passing through them are 0.130(6), –0.135(7), 0.130(7), and –0.124(9) Å, respectively, for **2A** and –0.194(6), 0.200(7), –0.190(7), and 0.184(7) Å, respectively, for **2B**. In **2A**, the deviation of the copper atom from this plane is rather high (0.117(3) Å), directed toward the coordinated N1B, as is expected for a square-pyramidal geometry. The Addison parameter ( $\tau$ ) of Cu is 0.20. However, the copper atom deviates only by 0.022(3) Å from the mean plane in **2B** with an angle of 9.39° between the planes N1B–Cu–O11B and N20B–Cu–N23B, indicating only a small tetrahedral distortion. The Cu···Cu distance within the dimer is 3.866 Å. In this compound, there is one weak intra-dimer C–H/ $\pi$  interaction between the H24E atom of molecule **B** and the phenyl ring of molecule **A** with dimensions C24B–H24E···CG 2.97 Å and  $\gamma = 20.4^\circ$ . There are also two other inter-dimer interactions: one between H19A from molecule **A** and the phenyl ring of **B** (0.5+*x*, 0.5–*y*, 0.5+*z*) and the other between H19F from molecule **B** and the phenyl ring of **A** (–0.5+*x*, 0.5–*y*, –0.5+*z*) with dimensions C19A–H19A···CG 2.74 Å,  $\gamma = 7.6^\circ$  and C19B–H19F···CG 2.93 Å,  $\gamma = 9.5^\circ$ . These C–H/ $\pi$  interactions form a one-dimensional chain along the *b* direction, as illustrated in Figure 2b.

It is to be noted that compounds **1** and **2** are polymerized isomers: **1** is a monomer and **2** is a dimer. There are several examples of polymerized isomers in coordination chemistry,<sup>19</sup> but in azido-bridged systems transformation

(19) Haddad, S. F.; Piekardt, J. *Transition Met. Chem.* **1993**, *18*, 377.

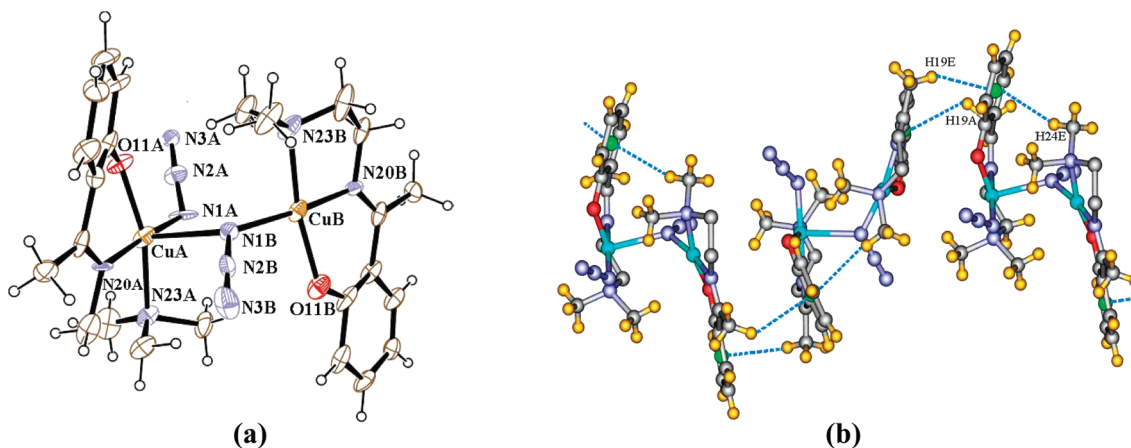


**Figure 2.** Structure of complex **2**. (a)  $\text{Cu}_2$  dimer with ellipsoids at 30% probability. (b) Polymeric 1D structure of **2** formed by the interdimer C–H/ $\pi$  interactions, shown as dotted lines.

between the isomers (**2** to **1** and **1** to **2**) is very rare. In the present system, the isomerization takes place only in solution. The TG/DSC study of compounds **1** and **2** does not show any interconversion in the solid state before decomposition (195 °C) (Figure S3). A unique feature of compound **2** is that it is a single-azido-bridged dimer. In fact, although there are several Cu(II)-azide compounds with this type of NNO Schiff base ligand, in most cases the compounds are double asymmetric EO azide-bridged dimers,<sup>14,5c,5d</sup> and the only example of a single bridged azido complex is not a dimer but a polymer.<sup>15b</sup>

**Structure of  $[\text{Cu}_7\text{L}_2(\text{N}_3)_{12}]_n$  (**3**).** The structure of compound **3**,  $\text{Cu}_7\text{L}_2(\text{N}_3)_{12}$ , is more complicated than that of **1** or **2** since there are four independent copper atoms in the asymmetric unit, three in general positions and one, namely Cu4, on an inversion center. Bond distances and angles are given in Table 3. There is only one independent Schiff base ligand, but the structure is completed with as many as six independent azide anions (Figure 3). Cu1 has a coordination geometry similar to that observed in **1** and **2** in that it is bonded to the three donor atoms of the ligand, O11, N20, and N23, and to an azide nitrogen atom, N1, in a nearly planar geometry. The only difference is the presence of an additional azide ligand coordinated through N7 in an axial position with a long Cu–N bond distance (2.357(10) Å), giving rise to a square-pyramidal geometry for Cu1. The basal plane has a rms deviation of 0.036 Å with the copper atom 0.059(7) Å from the plane in the direction of N7, as usually observed in square-pyramidal Cu(II) complexes. In addition, N7 is bridged to Cu2, while O11 and N1 are both bridged to Cu3. The coordination sphere of Cu2 consists of four azides in a basal plane, all of which bridge to other copper atoms. Thus, N13 and N16 are bonded to Cu4, N4 is bonded to Cu3, and, as stated above, N7 is bonded to Cu1. The square-pyramidal geometry around Cu2 is completed by N9<sup>a</sup> (<sup>a</sup> =  $-x, 2-y, 2-z$ ), which occupies an axial position with a long Cu–N bond distance of 2.336(11) Å. The rms deviation of donor atoms in the basal plane is 0.044 Å with Cu2 0.194(6) Å from this plane in the direction of the axial N9 atom. The azide N7–N8–N9 is the only one to bridge in a  $\mu$ -1,1,3 fashion. As can be seen from Figures 3 and 4, two such azides bridge two Cu2 atoms across a center of symmetry. Cu3

**Table 3.** Selected Bond Lengths (Å) and Bond Angles (deg) for Complex **3**

bond	distance (Å)	bond	angle (deg)
Cu1–N1	1.968(8)	N13–Cu2–N4	96.4(4)
Cu1–O11	1.925(8)	N13–Cu2–N9 <sup>a</sup>	91.9(4)
Cu1–N20	1.947(10)	N13–Cu2–N16	77.4(4)
Cu1–N23	1.997(11)	N4–Cu2–N9 <sup>a</sup>	96.4(4)
Cu1–N7	2.357(10)	N4–Cu2–N16	165.1(4)
Cu2–N7	2.000(9)	N9 <sup>a</sup> –Cu2–N16	97.3(4)
Cu2–N4	2.008(8)	N7–Cu2–N13	166.7(4)
Cu2–N9 <sup>a</sup>	2.336(11)	N7–Cu2–N4	92.6(4)
Cu2–N13	1.977(9)	N7–Cu2–N9 <sup>a</sup>	96.8(4)
Cu2–N16	2.002(8)	N7–Cu2–N16	91.5(4)
Cu3–N4	1.946(11)	O11–Cu1–N20	91.1(4)
Cu3–N10	1.963(9)	N7–Cu1–O11	88.2(3)
Cu3–O11	1.991(7)	N7–Cu1–N20	97.0(4)
Cu3–N10 <sup>b</sup>	2.006(10)	N7–Cu1–N23	97.6(5)
Cu3–N1	2.242(10)	N7–Cu1–N1	88.8(4)
Cu4–N16	1.917(10)	O11–Cu1–N23	174.1(5)
Cu4–N13	1.977(8)	N20–Cu1–N23	87.9(4)
		O11–Cu1–N1	83.5(4)
		N20–Cu1–N1	172.0(4)
		N23–Cu1–N1	96.9(4)
		N4–Cu3–N10	100.8(4)
		N4–Cu3–O11	88.6(3)
		N4–Cu3–N1	106.4(4)
		N4–Cu3–N10 <sup>b</sup>	161.0(4)
		N10–Cu3–O11	170.4(4)
		N10–Cu3–N1	99.9(4)
		N10–Cu3–N10 <sup>b</sup>	78.2(4)
		O11–Cu3–N1	75.3(3)
		O11–Cu3–N10 <sup>b</sup>	93.5(3)
		N1–Cu3–N10 <sup>b</sup>	92.4(4)
		N13–Cu4–N16	79.4(4)

<sup>a</sup>Symmetry elements =  $-x, 2-y, 2-z$ . <sup>b</sup>Symmetry elements =  $-x, 1-y, 2-z$ .

shows a square-pyramidal geometry, where the axial position is occupied by an azide N atom, N1, at 2.242(10) Å that bridges Cu3 to Cu1. The basal plane contains three azide N atoms: N4 connecting Cu3 with Cu2 and two N10 (from two equivalent azide ligands) connecting Cu3 with its symmetry-related Cu3 ion. The fourth basal position is occupied by the O11 atom from the Schiff base ligand, which connects Cu3 to Cu1 (Figure 3). Here the basal plane is quite distorted, with a rms deviation of 0.194 Å. As is found for the other Cu(II) ions, Cu3 is displaced from the basal plane toward the axial position by 0.133(4) Å. Cu4 is located on an inversion center and has a square-planar environment with four N atoms from four



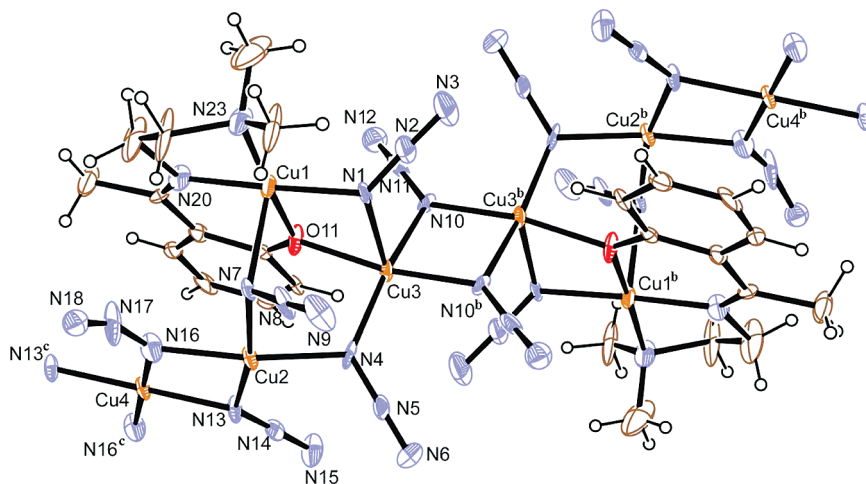


**Figure 3.** Centrosymmetric fragment of the polymeric structure of **3** with ellipsoids at 30% probability. Atoms Cu4 are positioned on additional centers of symmetry. Symmetry transformation:  $^b = -x, 1-y, 2-z$ ,  $^c = 1-x, 2-y, 2-z$ .

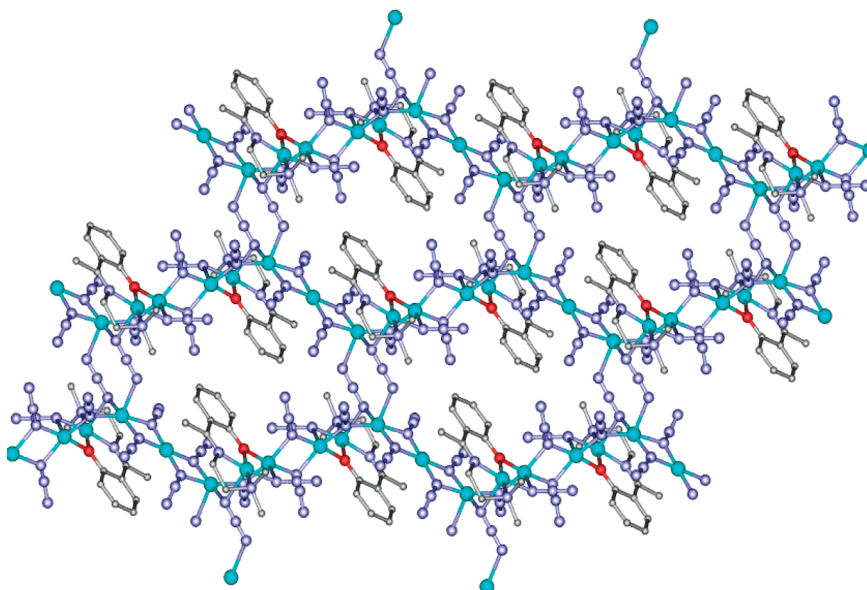


**Figure 4.** 2D polymeric structure of compound **3**. Hydrogen atoms are omitted for clarity. Color code: Cu = light blue, N = dark blue, O = red, C = white.

azide ligands, two N13 and two N16, connecting each Cu4 ion with its two Cu2 neighbors.

In summary, five of the six independent azide ligands act as  $\mu$ -1,1- $N_3$  bridges, Cu1–N1–Cu3, Cu2–N4–Cu3, Cu3–N10–Cu3, Cu2–N13–Cu4, and Cu2–N16–Cu4, giving rise to a one-dimensional zigzag chain along the crystallographic  $b$  axis. The only  $\mu$ -1,1,3- $N_3$  bridge is N7–N8–N9, which connects two Cu3 atoms of neighboring chains, forming a two-dimensional polymeric structure, as shown in Figure 4. Two of the  $\mu$ -1,1- $N_3$  ligands are disordered at the terminal nitrogen atom, viz., N12 and N18, and in both cases two sites were refined, each with occupancies of  $x$ ,  $1-x$ , with  $x$  refining to 0.66(2) and 0.51(2), respectively.

The overall structure of compound **3** can be viewed as formed by five  $\text{Cu}(\text{N}_3)_2$  and two  $[\text{Cu}(\text{L})(\text{N}_3)]$  units (identical to compound **1**), which are connected through phenoxo and  $\mu$ -1,1 and  $\mu$ -1,1,3 azido bridges to form the unprecedented two-dimensional structure shown in Figure 4. In this context, it should be mentioned that the common strategies for the extension of metal-azido assemblies are to introduce a

second bridging ligand (e.g., carboxylate)<sup>20</sup> or by employing chelating diamine ligands, such as ethylenediamine and its derivatives,<sup>6,21</sup> or the use of more azido ligands by adding a counteranion, such as  $\text{Cs}^+$  or  $\text{N}(\text{CH}_3)_4^+$ .<sup>22</sup> As far as we know, complex **3** is the first example where a mononuclear copper(II) Schiff base complex is extended to a 2D coordination polymer by simply introducing copper(II) azide. In this structure the Cu(II) ions are present in both square-planar and square-pyramidal geometries, demonstrating the flexibility of Cu(II) with coordination numbers four and five.

**Structure of  $[\text{Cu}_2\text{L}(\text{dmen})(\text{N}_3)_3]_n$  (**4**).** As mentioned earlier, the structure of **4** has already been reported.<sup>8</sup> So we

(20) Chen, Z.-L.; Jiang, C.-F.; Yan, W.-H.; Liang, F.-P.; Batten, S. R. *Inorg. Chem.* **2009**, *48*, 4674, and references therein.

(21) Gu, Z.-G.; Zuo, J.-L.; You, X.-Z. *Dalton Trans.* **2007**, 4067.

(22) (a) Góher, M. A. S.; Cano, J.; Journaux, Y.; Abu-Youssef, M. A. M.; Mautner, F. A.; Escuer, A.; Vicente, R. *Chem.—Eur. J.* **2000**, *6*, 778. (b) Mautner, F. A.; Cortes, R.; Lezama, L.; Rojo, T. *Angew. Chem., Int. Ed.* **1996**, *35*, 78. (c) Mautner, F. A.; Hanna, S.; Cortes, R.; Lezama, L.; Barandika, M. G.; Rojo, T. *Inorg. Chem.* **1999**, *38*, 4647.



**Table 4.** Selected Bond Lengths (Å) and Bond Angles (deg) for Complex 4

bond	distance (Å)	bond	angle (deg)
Cu1–N1	1.994(4)	N7–Cu2–N34	89.8(2)
Cu1–O11	1.902(3)	N4–Cu2–N34	174.1(2)
Cu1–N20	1.963(4)	N31–Cu2–N3 <sup>a</sup>	91.8(2)
Cu1–N23	2.049(4)	N7–Cu2–N3 <sup>a</sup>	95.5(2)
Cu1–N9	2.406(5)	N4–Cu2–N3 <sup>a</sup>	91.9(2)
Cu2–N31	1.985(4)	N34–Cu2–N3 <sup>a</sup>	92.3(2)
Cu2–N7	1.987(4)	N31–Cu2–N7	171.0(2)
Cu2–N4	1.999(4)	N31–Cu2–N4	91.1(2)
Cu2–N34	2.089(4)	N7–Cu2–N4	94.0(2)
Cu2–N3 <sup>a</sup>	2.440(5)	N31–Cu2–N34	84.6(2)
		O11–Cu1–N20	92.5(2)
		O11–Cu1–N23	172.2(2)
		N20–Cu1–N23	84.9(2)
		O11–Cu1–N1	91.4(2)
		N20–Cu1–N1	162.1(2)
		N23–Cu1–N1	88.9(2)

<sup>a</sup> Symmetry elements =  $x, -1+y, z$ .

do not describe the structure in detail here. However our crystallographic data are better, as the previous data were collected at room temperature and only to a  $2\theta$  max of  $50^\circ$ . In addition there are significant differences in the cell parameters, so we include the structural parameters in Table 1 and bond distances and angles in Table 4. One point that was missed by the previous authors is that the  $\mu$ -1,1- $N_3$  azide bridges lead to a helical chain, as can be seen in Figures 5 and 6, where Cu1 and Cu2 atoms are connected through basal-axial  $\mu$ -1,3- $N_3$  bridges. These chains are connected through long asymmetric  $\mu$ -1,1- $N_3$  bridges between two Cu2 ions of different chains and through two intermolecular H-bonds, forming the double-helical chain (Figures 5 and 6).

It is interesting to note that although several  $\mu$ -1,3- $N_3$ -bridged helical chains have been reported with Mn(II/III) and Ni(II),<sup>23–25</sup> there are very few examples of such helical chains with Cu(II). In fact, a careful search in the CCDC database shows that there are only three Cu(II) chains connected through single  $\mu$ -1,3- $N_3$  bridges,<sup>26</sup> and only one of these<sup>26a</sup> presents a helical structure (the other two are zigzag chains), although it has not been magnetically characterized. Therefore, compound **4** is the first magnetically characterized example of a helical Cu(II) chain connected through a single  $\mu$ -1,3- $N_3$  bridge.

### Magnetic Properties

[CuL( $N_3$ )] (**1**). The thermal variation of the molar magnetic susceptibility per two Cu(II) ions times the temperature ( $\chi_m T$ ) for compound **1** shows at room temperature a value of ca.  $0.80 \text{ emu} \cdot \text{K} \cdot \text{mol}^{-1}$ , the expected value for two isolated Cu(II)  $S = 1/2$  ions with  $g \approx 2.07$  (Figure 7). On cooling the sample, the  $\chi_m T$  product remains constant down to ca. 15 K. Below this tempera-

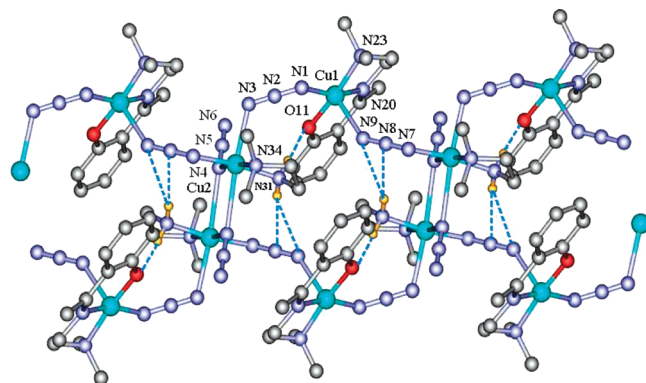


**Figure 5.** Two 1D chains in **4** connected through long asymmetric  $\mu$ -1,1- $N_3$  bridges and H-bonds (shown as dotted lines). All hydrogen atoms, except the amine ones implicated in the H-bonds, are omitted for clarity. Color code: Cu = light blue, N = dark blue, O = red, C = black, H = yellow.

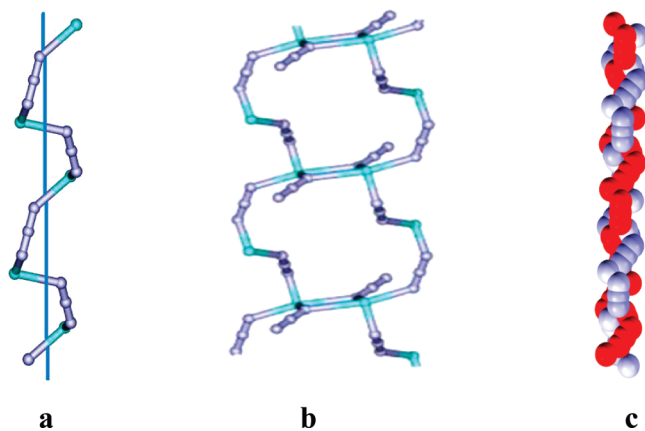


**Figure 6.** Helical structure of complex **4**: (a) Single 1D helical chain; (b) two helical chains through long asymmetric  $\mu$ -1,1- $N_3$  bridges; (c) space-filling view of a single helical chain.

ture,  $\chi_m T$  shows an abrupt decrease, reaching a value of ca.  $0.48 \text{ emu} \cdot \text{K} \cdot \text{mol}^{-1}$  at 2 K. This behavior indicates that compound **1** presents a weak antiferromagnetic coupling, responsible for the observed decrease of  $\chi_m T$  at low temperatures.

Although the structure of this compound shows the presence of Cu(II) monomers, a closer inspection shows that each monomer has a close, symmetry-related, neighbor (**1A** and **1B**, see Figure 1b) that presents a close C–H/ $\pi$  contact from a methyl group of **1B** to a phenyl ring of **1A**. Accordingly, we have fitted the magnetic properties to the simple Bleaney–Bowers  $S = 1/2$  dimer model.<sup>27</sup> This model reproduces very satisfactorily the magnetic properties of compound **1** (solid line in Figure 7) with  $g = 2.085(2)$  and  $J = -1.77(2) \text{ cm}^{-1}$  (Table 5, the Hamiltonian is written as  $H = -JS_1S_2$ ). As expected, the weak antiferromagnetic coupling observed in compound **1** is confirmed by the isothermal magnetization that shows, at 2 K and 5 T, a value of ca.  $1.2 \mu_B$ , well below the expected one for two noninteracting Cu(II) ions (Figure 8).

[CuL( $N_3$ )]<sub>2</sub> (**2**). The thermal variation of the molar magnetic susceptibility per Cu(II) dimer times the temperature

(23) (a) Ko, H. H.; Lim, J. H.; Kim, H. C.; Hong, C. S. *Inorg. Chem.* **2006**, 45, 8847. (b) Yuan, M.; Zhao, F.; Zhang, W.; Wang, Z.-M.; Gao, S. *Inorg. Chem.* **2007**, 46, 11235.

(24) Reddy, K. R.; Rajasekharan, M. V.; Tuchagues, J. P. *Inorg. Chem.* **1998**, 37, 5978.

(25) (a) Monfort, M.; Ribas, J.; Solans, X.; Font-Bardía, M. *Inorg. Chem.* **1996**, 35, 7633. (b) Ftibas, J.; Monfort, M.; Diaz, C.; Bastos, C.; Mer, C.; Solans, X. *Inorg. Chem.* **1995**, 34, 4986.

(26) (a) Cabort, A.; Therrien, B.; Bernauer, K.; Süss-Fink, G. *Inorg. Chim. Acta* **2003**, 349, 78. (b) Adhikary, C.; Mal, D.; Okamoto, K.; Chaudhuri, S.; Koner, S. *Polyhedron* **2006**, 25, 2191. (c) Yuan, C. L. *Acta Crystallogr. Sect. E* **2007**, 63, m3148.

(27) (a) Bleaney, B.; Blowers, K. D. *Proc. R. Soc. (London) Ser. A* **1952**, 214, 451. (b) Kahn, O. *Molecular Magnetism*; VCH Publishers, 1993.

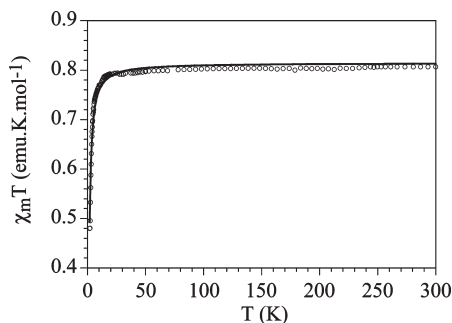


**Figure 7.** Thermal variation of the  $\chi_m T$  product for compound **1**. The solid line shows the best fit to the  $S = 1/2$  dimer model (see text).

**Table 5.** Structural and Magnetic Parameters of Compounds 1–4

compound	structure	bridge(s)	$g$	$J$ (cm <sup>-1</sup> )
<b>1</b>	Cu-dimer	C–H/ $\pi$ -overlap	2.085	–1.77
<b>2</b>	Cu-dimer	single 1,1'-N <sub>3</sub> (asymmetric)	2.102	–1.97
<b>3</b>	Cu-chain	double 1,1'-N <sub>3</sub> (symmetric)	2.110	20.1
		single 1,1'-N <sub>3</sub> (symmetric)		–68.1
		single oxo (symmetric)		–4.0
<b>4</b>	Cu-chain	single 1,3-N <sub>3</sub> asymmetric	2.186	–1.35
		single 1,3-N <sub>3</sub> asymmetric		–2.64

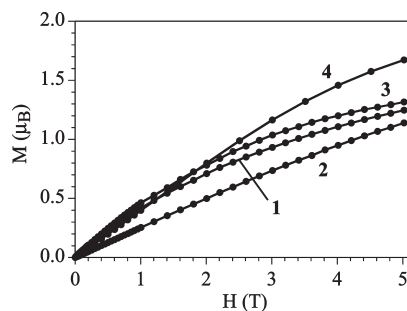


**Figure 8.** Isothermal magnetization at 2 K for compounds **1** (per Cu<sub>2</sub> unit), **2** (per Cu<sub>2</sub> unit), **3** (per Cu<sub>7</sub> unit), and **4** (per Cu<sub>2</sub> unit).

( $\chi_m T$ ) for compound **2** shows at room temperature a value of ca. 0.82 emu·K·mol<sup>-1</sup>, expected for two isolated Cu(II)  $S = 1/2$  ions with  $g = 2.09$  (Figure 9). When cooling the sample,  $\chi_m T$  remains constant down to ca. 50 K and shows a progressive decrease below this temperature to reach a value of ca. 0.50 emu·K·mol<sup>-1</sup> at ca. 2 K (Figure 9). This behavior indicates that compound **2** also presents a weak antiferromagnetic coupling, responsible for the progressive decrease observed below ca. 50 K.

Since the structure of this compound shows the presence of Cu(II) dimers in which the Cu(II) ions are connected through a long and asymmetric 1,1'-N<sub>3</sub> bridge (Figure 2a), we have fitted the magnetic properties of this compound to the Bleaney–Bowers dimer model for two  $S = 1/2$  ions.<sup>27</sup> This simple model reproduces very satisfactorily the magnetic properties of compound **2** in the whole temperature range (solid line in Figure 9) with  $g = 2.102(2)$  and  $J = -1.97(3)$  cm<sup>-1</sup> (Table 5, the Hamiltonian is written as  $H = -JS_1S_2$ ). Confirmation of the weak antiferromagnetic coupling found in compound **2** is provided by the isothermal magnetization at 2 K that shows almost a linear field dependence, without reaching saturation at 5 T (Figure 8). At 5 T the magnetization value is ca. 1.2  $\mu_B$ , well below the expected one for two noninteracting  $S = 1/2$  Cu(II) ions (2  $\mu_B$ ), confirming

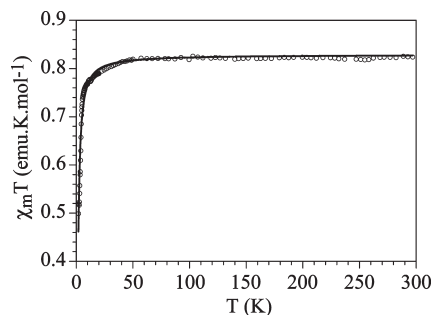


**Figure 9.** Thermal variation of the  $\chi_m T$  product per Cu(II) dimer for compound **2**. The solid line shows the best fit to the  $S = 1/2$  dimer model (see text).

the presence of antiferromagnetic interactions in this compound.

[Cu<sub>7</sub>L<sub>2</sub>(N<sub>3</sub>)<sub>12</sub>]<sub>n</sub> (**3**). The thermal variation of the molar magnetic susceptibility per seven Cu(II) ions times the temperature ( $\chi_m T$ ) for compound **3** shows at room temperature a value of ca. 2.70 emu·K·mol<sup>-1</sup>, close to that expected for seven isolated Cu(II)  $S = 1/2$  ions with  $g = 2$  (Figure 10). When cooling the sample, the  $\chi_m T$  product shows a continuous decrease to reach a value of ca. 2.5 emu·K·mol<sup>-1</sup> at ca. 50 K and then a smoothness until 20 K (Figure 10). Below ca. 20 K the  $\chi_m T$  product shows a more abrupt decrease to reach a value of ca. 1.2 emu·K·mol<sup>-1</sup> at 2 K. This behavior indicates the presence of predominant antiferromagnetic interactions in this compound.

Since the structure of this compound shows a complex 2D structure with six different azide bridges, we have necessarily made some approximations in order to fit the magnetic properties. In a first step we have discarded the interchain connection (through a long Cu–N bond of 2.336(11) Å) and the Cu1–Cu2 asymmetric azide bridge (through a long Cu–N bond of 2.357(10) Å) since they are the weakest ones. In this way, we can fit the magnetic data to an alternating decorated chain, as indicated in the inset of Figure 10. Since even this simplified model implies the presence of up to four different exchange constants, in a second approach we have assumed that the coupling constant through Cu2–Cu4 ( $J_{24}$ ) is equal to that through Cu3–Cu3 ( $J_{33}$ ). This assumption is based on the fact that both double 1,1'-N<sub>3</sub> bridges show very similar structural parameters such as Cu–N bond distances and Cu–N–Cu bond angles; see below. With these simplifications it is possible to reproduce the magnetic properties of compound **3** by using a 14 Cu(II) center closed-chain model,<sup>28</sup> corresponding to two heptameric units –Cu2–Cu4–Cu2–Cu3[Cu1]–Cu3[Cu1]– (solid line in Figure 10) with the following set of parameters:  $g = 2.110$ ,  $J_{24} = J_{33} = 20.1$  cm<sup>-1</sup> (corresponding to the double 1,1'-N<sub>3</sub> bridges),  $J_{23} = -68.1$  cm<sup>-1</sup> (corresponding to the single 1,1'-N<sub>3</sub> bridge), and  $J_{13} = -4.0$  cm<sup>-1</sup> (corresponding to the single oxo bridge, Table 5). This model reproduces very satisfactorily the magnetic properties of compound **3** in the temperature range 300–30 K. Below this temperature the experimental points are below the theoretical

(28) (a) Borrás-Almenar, J. J.; Clemente-Juan, J. M.; Coronado, E.; Lloret, F. *Chem. Phys. Lett.* **1997**, 275, 79. (b) Borrás-Almenar, J. J.; Clemente-Juan, J. M.; Coronado, E.; Tsukerblat, B. S. *Inorg. Chem.* **1999**, 38, 6081. (c) Borrás-Almenar, J. J.; Clemente-Juan, J. M.; Coronado, E.; Tsukerblat, B. S. *J. Comput. Chem.* **2001**, 22, 985.

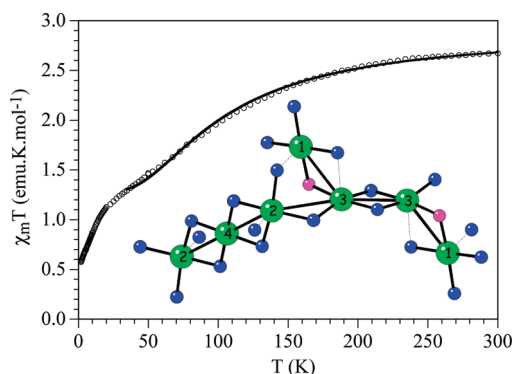


**Figure 10.** Thermal variation of the  $\chi_m T$  product per seven Cu(II) ions for compound **3**. The solid line shows the best fit to the  $S = 1/2$  chain model (see text). Inset shows the exchange pathways considered in the model.

ones, indicating, as expected, the presence of additional antiferromagnetic interactions (mainly those that were neglected in the first step). Unfortunately, the presence of so many different exchange pathways precludes a more accurate fit of the magnetic properties.

The antiferromagnetic nature of the coupling found in compound **3** is also observed in the isothermal magnetization at 2 K, which shows no saturation at 5 T with a magnetization value of ca.  $1.4 \mu_B$  per Cu<sub>7</sub> unit (Figure 8), well below the expected one for seven noninteracting  $S = 1/2$  Cu(II) ions (ca.  $7 \mu_B$ ).

**[Cu<sub>2</sub>L(dmen)(N<sub>3</sub>)<sub>3</sub>]<sub>n</sub> (4).** The thermal variation of the molar magnetic susceptibility per two Cu(II) ions times the temperature ( $\chi_m T$ ) for compound **4** shows at room temperature a value of ca.  $0.90 \text{ emu} \cdot \text{K} \cdot \text{mol}^{-1}$ , a value close to that expected for two isolated Cu(II)  $S = 1/2$  ions with  $g \approx 2.19$  (Figure 11). When cooling the sample, the  $\chi_m T$  product remains constant down to ca. 10 K. Below this temperature,  $\chi_m T$  shows an abrupt decrease, reaching a value of ca.  $0.44 \text{ emu} \cdot \text{K} \cdot \text{mol}^{-1}$  at 2 K. This behavior indicates that compound **4** presents a weak antiferromagnetic coupling, responsible for the observed decrease of  $\chi_m T$  at low temperatures.

Since the structure of this compound shows the presence of a Cu(II) chain formed by two different Cu(II) ions, Cu1 and Cu2, connected through two different asymmetric alternating 1,3-N<sub>3</sub> bridges (–N1–N2–N3– and –N7–N8–N9–, Figure 5), we can use two different models to reproduce the magnetic properties. First, if we assume that the two bridges are equivalent, then we can use the regular  $S = 1/2$  antiferromagnetic chain model derived by Hatfield et al.<sup>29</sup> Unfortunately, this model is not able to reproduce the magnetic properties adequately, no doubt because of significant variations in the bridging angles (see below), and therefore we have used a second model involving alternating  $S = 1/2$  antiferromagnetic chains, also derived by Hatfield et al.<sup>30</sup> This model reproduces very satisfactorily the magnetic properties of compound **4** (the solid line in Figure 11) with the following set of parameters:  $g = 2.1858(7)$ ,  $J_1 = -1.35(1) \text{ cm}^{-1}$  and  $J_2 = -2.64(1) \text{ cm}^{-1}$  ( $\alpha = |J_2|/|J_1| =$

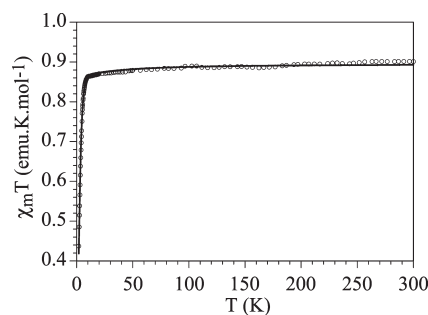


**Figure 11.** Thermal variation of the  $\chi_m T$  product for compound **4**. Solid line shows the best fit to the alternating  $S = 1/2$  chain model (see text).

$1.958(6)$  (Table 5); the Hamiltonian is written as  $H = -JS_i S_j$ ). As in the other compounds, the isothermal magnetization measurements at 2 K (Figure 8) confirm the presence of a weak antiferromagnetic coupling. Thus, at 2 K, compound **4** shows an almost linear dependence of the magnetization on the magnetic field and no saturation for fields of 5 T. The magnetization value at 2 K per Cu(II) dimer (ca.  $1.7 \mu_B$ ) is below expected for two noninteracting Cu(II) ions (ca.  $2.0 \mu_B$ ), confirming the presence of weak antiferromagnetic interactions.

The antiferromagnetic couplings found in the four compounds can be readily explained from the magnetostructural correlations established for 1,1-N<sub>3</sub> and 1,3-N<sub>3</sub> symmetric and asymmetric bridges.<sup>31,5c,5i</sup> Thus, the weak antiferromagnetic coupling found in compound **1** can be attributed to the close C–H/ $\pi$  contact from a methyl group of monomer **1B** to a phenyl ring of the monomer **1A**. This interaction is expected to give rise to a weak antiferromagnetic coupling, in agreement with the experimental results.

Compound **2** presents a Cu(II) dimer with an asymmetric 1,1'-N<sub>3</sub> bridge (Figure 2a). DFT calculations performed on this kind of bridge show that for a long Cu–N bond distance of ca. 2.53 Å the expected coupling should be ca.  $-5 \text{ cm}^{-1}$  for a double bridge (ca.  $-2.5 \text{ cm}^{-1}$  for a single one), in agreement with the experimental value obtained in this compound (Table 5).

Compound **3** has a much more complex structure since there are six different bridges connecting the four independent Cu(II) ions. Nevertheless, as already mentioned, we can, in a first approach, assume that the long asymmetric azide bridges are negligible as compared with the short and symmetric ones, and, thus, the coupling scheme is reduced to only four different coupling constants. A further simplification can be made if we assume that the structural parameters of the two double 1,1'-N<sub>3</sub> bridges connecting Cu2–Cu4 and Cu3–Cu3 are very similar (see Figure 12), and in order to reduce the number of adjustable parameters, we can assume that they are equivalent. As already explained above, the two other bridges are a symmetrical single 1,1-N<sub>3</sub> bridge, connecting the Cu2 and Cu3 atoms (Figure 12), and a single oxo bridge that connects, together with an asymmetric 1,1'-N<sub>3</sub> bridge, the Cu1 and Cu3 atoms (Figure 12).

(29) Brown, D. B.; Donner, J. A.; Hall, J. W.; Wilson, S. R.; Wilson, R. B.; Hodgson, D. J.; Hatfield, W. E. *Inorg. Chem.* **1979**, *18*, 2635.

(30) Hall, J. W.; Marsh, W. E.; Weller, R. R.; Hatfield, W. E. *Inorg. Chem.* **1981**, *20*, 1033.

(31) (a) Triki, S.; Gómez-García, C. J.; Ruiz, E.; Sala-Pala, J. *Inorg. Chem.* **2005**, *44*, 5501. (b) Ruiz, E.; Cano, J.; Alvarez, S.; Alemany, P. *J. Am. Chem. Soc.* **1998**, *120*, 11122. (c) Fabrizi de Biani, F.; Ruiz, E.; Cano, J.; Novoa, J. J.; Alvarez, S. *Inorg. Chem.* **2000**, *39*, 3221.



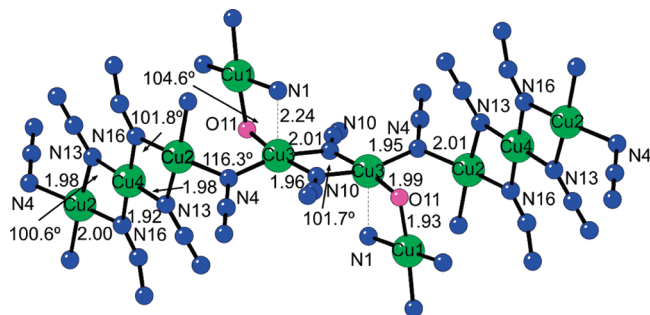


**Figure 12.** View of the coordination environment of the Cu(II) ions in compound **3** showing the bridging bond distances (in Å) and angles (in deg). Color code: Cu = green, N = blue, O = pink.

The weak antiferromagnetic coupling found for the single oxo bridge ( $-4.0 \text{ cm}^{-1}$ ) can be easily rationalized from the magnetostructural correlations that predict a weak antiferromagnetic coupling for this kind of bridge.<sup>32</sup> The additional asymmetric  $1,1'-\text{N}_3$  bridge connecting the Cu1 and Cu3 atoms is also expected to give rise to a weak antiferromagnetic coupling given the long Cu–N bond distance.<sup>31</sup> The single symmetric  $1,1'-\text{N}_3$  bridge connecting the Cu2 and Cu3 atoms is more difficult to correlate since this is a very rare  $1,1'-\text{N}_3$  bridge with a very large Cu–N–Cu bond angle ( $116.3^\circ$ ). This angle is expected to lead to strong antiferromagnetic coupling, but the big dihedral angle between the basal planes of the two Cu(II) ions connected through this bridge, Cu2 with Cu3, is expected to significantly reduce the antiferromagnetic coupling constant, leading to the observed moderate coupling ( $-68.1 \text{ cm}^{-1}$ ). Finally, for the double  $1,1'-\text{N}_3$  bridges connecting Cu2 with Cu4 and Cu3 with the other symmetry-related Cu3 ion, magnetostructural correlations and DFT calculations show that the two main parameters determining the sign and magnitude of the exchange coupling are the Cu–N bond distances and the Cu–N–Cu bond angles.<sup>31b</sup> In the case of the  $1,1-\text{N}_3$  bridges of compound **3**, the Cu–N bond distances (in the range  $1.92\text{--}2.01 \text{ Å}$ , see Figure 12) and the Cu–N–Cu bond angles (in the range  $100.6\text{--}101.8^\circ$ ) indicate that the exchange coupling through these bridges should be ca.  $20 \text{ cm}^{-1}$ , in very good agreement with experiment.

The magnetic couplings found in compound **4** are also easy to explain since the asymmetric  $1,3-\text{N}_3$  bridge is well known to originate weak antiferromagnetic couplings.<sup>5e,i</sup> Thus, the correlation established for asymmetric  $1,3-\text{N}_3$  bridges based on DFT calculations indicate that the coupling constant mainly depends on the long Cu–N bond distance.<sup>31a</sup> For bond distances in the range  $2.4\text{--}2.5 \text{ Å}$  this coupling is expected to be antiferromagnetic

and very weak (of a few  $\text{cm}^{-1}$ ), in agreement with the experimental results. Furthermore, since this correlation indicates that the longer the Cu–N bond distance, the weaker the magnetic coupling, we can attribute the weaker coupling constant ( $-1.35 \text{ cm}^{-1}$ ) to the longer Cu2–N3 bond ( $2.440(5) \text{ Å}$ ) and the stronger one ( $-2.64 \text{ cm}^{-1}$ ) to the shorter Cu1–N9 bond ( $2.406(5) \text{ Å}$ ).

## Conclusions

The rational synthesis of compounds **1–4** constitutes a rare example where subtle changes in the synthetic conditions (such as the crystallization temperature or the Cu(II) precursor) or the Cu(II)/HL/ $\text{N}_3^-$  ratio lead to a monomer, a dimer, a helical chain, and a hexagonal layer with the same Schiff base ligand. Even more exceptional is the fact that the four complexes can easily be interconverted in solution. The structures of compounds **1** and **2** show that they differ only in the presence of a weak asymmetric  $1,1-\text{N}_3$  bridge in the dimer **2**. It seems that lower temperatures facilitate such association. The composition and structure of **3** demonstrate that a complex polymeric structure can be obtained by simply inserting Cu(II) azide into a mononuclear Schiff base complex. The bridging ability of the phenoxo oxygen atom together with the flexible coordination modes of azide and the coordination flexibility of Cu(II) play an important role in the formation of such an atypical structure. The magnetic couplings in compounds **1** and **2** are weak and antiferromagnetic, in agreement with the close C–H/ $\pi$  contacts observed in **1** and the asymmetric  $1,1-\text{N}_3$  bridge present in **2**. Compound **3** is a unique example of an alternating and decorated azide-bridged copper chain presenting ferro- and antiferromagnetic couplings. The ferromagnetic coupling found in the two symmetric  $1,1-\text{N}_3$  bridges fully agrees with previous magnetostructural correlations and DFT calculations. On the other hand, the weak antiferromagnetic couplings found for the single  $1,1-\text{N}_3$  and oxo bridges also agree with the magnetostructural correlations in these kinds of bridges. Compound **4** presents alternating weak antiferromagnetic couplings, as expected for such asymmetric  $1,3-\text{N}_3$  bridges.

**Acknowledgment.** We thank CSIR, Government of India [Junior Research Fellowship to S.N., Sanction no. 09/028 (0702)/2008-EMR-I], the European Union (MAGMANet Network of Excellence), the Spanish Ministerio de Educación y Ciencia (Projects MAT2007-61584 and Consolider-Ingenio 2010 CSD 2007-00010 in Molecular Nanoscience), and the Generalitat Valenciana (Project PROMETEO/2009/095) for financial support. We also thank EPSRC and the University of Reading for funds for the X Calibur system.

**Supporting Information Available:** This material is available free of charge via the Internet at <http://pubs.acs.org>.

(32) Chiari, B.; Helms, J. H.; Piovesana, O.; Tarantelli, T.; Zanazzi, P. F. *Inorg. Chem.* **1986**, *25*, 2408.